# Inner-Shell Excitation of 3d Transition-Metal Carbonyls [$Mn_2(CO)_{10}$, $Mn(CO)_5Br$, and $Mn(CO)_5H$] Studied by Electron Energy Loss Spectroscopy

**E. Rühl[†] and A. P. Hitchcock***

*Contribution from the Department of Chemistry, McMaster University, Hamilton, Canada, L8S 4M1.* *Received September 9, 1988*

**Abstract:** The C 1s and O 1s spectra of $Mn_2(CO)_{10}$, $Mn(CO)_5Br$, and $Mn(CO)_5H$, along with the Mn 3p and Mn 2p spectra of $Mn_2(CO)_{10}$ and $Mn(CO)_5Br$, have been recorded with inelastic electron scattering under conditions dominated by electric dipole transitions. The C 1s and O 1s spectra, converted to absolute oscillator strength scales, are analyzed in comparison to those of free CO and of other metal carbonyls. The oscillator strengths of the carbon and oxygen 1s $\rightarrow \pi^*$ transitions are found to shift systematically with changes in the ligand and the transition metal, in a fashion consistent with the relative extent of $d\pi$-$p\pi$ back-bonding. In contrast, the relationship between 1s $\rightarrow \pi^*$ energies or term values and ground-state $d\pi$-$p\pi$ back-bonding is less direct because of differences in the relaxation (core hole polarization) of the core-excited and core-ionized states. The relationship between 1s $\rightarrow \sigma^*$ energies and C-O bond lengths is considered. It is found that the "main line" in photoemission does *not* provide a suitable reference for correlations between 1s $\rightarrow \sigma^*$ energies and C-O bond lengths. Alternate choices for reference energies are discussed.

## I. Introduction

The spectroscopy of transition metal carbonyl complexes has been studied extensively, since these compounds are important in homogeneous catalysis and are useful models for the interaction of CO with transition metal surfaces, an interaction directly relevant to heterogeneous catalysis. The occupied electronic structure of carbonyl systems has been extensively explored by, e.g., valence and core level photoelectron spectroscopy[1,2] and quantum chemistry,[3,4] while spectroscopic studies of the unoccupied levels include electron transmission spectroscopy (ETS)[5] and valence excitation in the visible and near-ultraviolet.[6]

A subject of active debate with regard to metal-carbonyl bonding is the relative contribution of $5\sigma$ donation versus $d\pi$-$p\pi$ back-bonding to the ground-state electronic structure of both metal-carbonyl complexes and surface-adsorbed CO. The "classical" Blyholder model[7] envisages relatively equal contributions. However, Bagus[3] has proposed that the $d\pi$-$p\pi$ contribution is more important, while Johnson and Klemperer[8] claim that $5\sigma$ donation dominates. Although shifts in carbonyl stretching frequencies and absolute intensities[7] have been a traditional measure of the relative strength of $d\pi$-$p\pi$ back-bonding, other techniques such as photoelectron,[9,10] inverse photoemission,[11] and Penning ionization[12] spectroscopies have also addressed this question in recent years. The ideal probe of $d\pi$-$p\pi$ back-bonding would provide a map of the ground-state electronic distribution in the metal-carbonyl bond within an orbital model.

Inner-shell excitation has potentially some special advantages in this regard. It measures a site-selected, dipole, partial density of states since the core hole localizes the excitation on a single atom. C 1s (O 1s) excitation samples primiarily the $C_{2p}$ ($O_{2p}$) contribution to the optical orbital. Thus 1s $\rightarrow \pi^*$ energies and particularly transition intensities, which are directly sensitive to the $C_{2p}$ and $O_{2p}$ contributions to the $\pi^*$ orbital, *could* be a useful probe of ($d\pi$-$p\pi$) back-bonding in transition metal-carbonyl complexes. This potential has motivated our study of the core excitation spectra of $Mn_2(CO)_{10}$, $Mn(CO)_5Br$, and $Mn(CO)_5H$. Our results complement recent high-resolution inner-shell electron energy loss (ISEELS) studies of $Ni(CO)_4$,[13] $Mo(CO)_6$, $Cr(CO)_6$, and $Fe(CO)_5$,[14] which have also addressed this subject. A potential limitation of core excitation as a probe of ground-state electronic structure is the possibility of distortions of the orbital of interest by the core hole. Avouris et al.[15] have calculated that significant reorganization of the $\pi^*$-orbital distribution occurs in both the ($C\ 1s,\pi^*$) and ($O\ 1s,\pi^*$) states. [Note: in our notation for configurations, italics indicates a vacancy.] If this effect is small, or at least constant throughout a molecular series, the intensities of transitions to a common virtual orbital ($\pi^*$) from a variety of different core levels (O 1s, C 1s, Mn np) can be used to map the relative changes in spatial distribution of that virtual orbital. Avanzino et al.[10] have concluded from their XPS studies that the *variations* in core hole relaxation effects through a series of 12 pentacarbonylmanganese compounds is no greater than 0.1 eV. The intensities of 1s $\rightarrow \pi^*$ transitions have been used recently to study the effects of various substituents on the spatial distributions of the carbonyl $\pi^*$ orbital in HCOX, X = F, OH, $NH_2$.[16]

[†] Permanent address: Institut für Physikalische Chemie, Freie Universität Berlin, Takustr. 3, D-1000 Berlin 33, Germany. Present address: Department of Chemistry, University of Colorado, Boulder, CO 80309.

(1) Plummer, E. W.; Salanek, W. R.; Miller, J. S. *Phys. Rev. B* **1978**, *18*, 1673. Plummer, E. W.; Eberhardt, W. *Adv. Chem. Phys.* **1982**, *49*, 533.
(2) Freund, H.-J.; Plummer, E. W. *Phys. Rev. B* **1981**, *23*, 4859.
(3) Bagus, P. S.; Nelin, C. J.; Bauschlicher, C. W. *Phys. Rev. B* **1983**, *28*, 5423. Bauschlicher, C. W.; Bagus, P. S. *J. Chem. Phys.* **1984**, *81*, 5889. Bagus, P. S.; Hermann, K. *Appl. Surf. Sci.* **1985**, *22/23*, 444.
(4) Baerends, E. J.; Ros, P. *Mol. Phys.* **1975**, *30*, 1735. Ziegler, T.; Rauk, A. *Inorg. Chem.* **1979**, *18*, 1755.
(5) Giordan, J. C.; Moore, J. H.; Tossell, J. A. *J. Am. Chem. Soc.* **1981**, *103*, 6632. Giordan, J. C.; Moore, J. H.; Tossell, J. A. *ACS Symp. Ser.* **1984**, *263*, 193. Giordan, J. C.; Moore, J. H.; Tossell, J. A. *Acc. Chem. Res.* **1986**, *19*, 281.
(6) Gray, H. B.; Beach, N. A. *J. Am. Chem. Soc.* **1963**, *85*, 2922. Beach, N. A.; Gray, H. B. *J. Am. Chem. Soc.* **1968**, *90*, 5713. Blakney, G. B.; Allen, W. F. *Inorg. Chem.* **1971**, *10*, 2763.
(7) Blyholder, G. *J. Phys. Chem.* **1964**, *68*, 2772. Cotton, F. A. *Inorg. Chem.* **1964**, *3*, 702. Cotton, F. A.; Wing, R. M. *Inorg. Chem.* **1965**, *4*, 314. Blyholder, G.; Allen, M. C. *J. Am. Chem. Soc.* **1969**, *91*, 3158. El-Mottaleb, M. S. A. A. *J. Mol. Struct.* **1975**, *25*, 438. Sheppard, N.; Nguyen, T. J. *Adv. Infrared Raman Spectrosc.* **1978**, *5*, 67.
(8) Johnson, J. B.; Klemperer, W. G. *J. Am. Chem. Soc.* **1977**, *99*, 7132.
(9) Smith, R. J.; Anderson, J.; Lapeyre, G. L. *Phys. Rev. B* **1980**, *22*, 632. Roussel, J.; Boiziau, C.; Nuvolone, R.; Reynaud, C. *Surf. Sci.* **1981**, *110*, L634.
(10) Chen, H. W.; Jolly, W. L.; Kopf, J.; Lee, T. H. *J. Am. Chem. Soc.* **1979**, *101*, 2607. Avanzino, S. C.; Bakke, A. A.; Chen, H. W.; Donahue, C. J.; Jolly, W. L.; Lee, T. H.; Ricco, A. J. *Inorg. Chem.* **1980**, *19*, 1931.
(11) Fauster, Th.; Himpsel, F. J. *Phys. Rev. B* **1983**, *27*, 1390. Gumhalter, B. *Surf. Sci.* **1985**, *157*, L355. Johnson, P. D.; Hulbert, S. L. *Phys. Rev. B* **1987**, *35*, 9427. Dose, V. *Surf. Sci. Rep.* **1985**, *5*, 337. Smith, N. V.; Woodruff, D. P. *Prog. Surf. Sci.* **1986**, *21*, 295.
(12) Boszo, F.; Arias, J.; Yates, J. T.; Martin, R. M.; Metiu, H. *Chem. Phys. Lett.* **1983**, *94*, 243.
(13) Cooper, G.; Sze, K. H.; Brion, C. E. *J. Am. Chem. Soc.*, submitted for publication.
(14) Cooper, G.; Sze, K. H.; Brion, C. E. unpublished work.
(15) Avouris, Ph.; Bagus, P. S.; Rossi, A. R. *J. Vac. Sci. Technol. B* **1985**, *3*, 1484.
(16) Ishii, I.; Hitchcock, A. P. *J. Chem. Phys.* **1987**, *87*, 830.

0002-7863/89/1511-2614$01.50/0 

**Table I.** Energies ($E$, eV), Term Values (TV, eV), and Proposed Assignments for Features in the C 1s Spectra of CO, $Mn_2(CO)_{10}$, $Mn(CO)_5Br$, and $Mn(CO)_5H$

| CO[a] | | $Mn_2(CO)_{10}$ | | $Mn(CO)_5Br$ | | $Mn(CO)_5H$ | | assignment (final orbital) |
|---|---|---|---|---|---|---|---|---|
| $E$ | TV[b] | $E$ | TV[b] | $E$ | TV[b] | $E$ | TV[b] | |
| 287.40[c] | 8.7 | 287.70[d] | 5.6 | 287.79[e] | 6.1 | 287.85[f] | 6.0 | $\pi^*$ |
| | | 289.5 | 3.8 | 290.3 | 3.4 | 289.7 | 4.1 | $\pi^*$(delocal); $\sigma^*$(Mn–C) |
| 292.54 | 3.4 | 290.7 | 2.6 | 291.1 | 3.0 | 290.7 | 3.1 | "3s" Ryd |
| 293.32 | 2.6 | 291.5 | 1.8 | 292.1 | 2.0 | 291.1 | 2.7 | "3p" Ryd |
| | | 292.1 | 1.2 | | | 292.3 | 1.5 | |
| 296.1 | | 293.3[g] | | 294.1[h] | | 293.8[g] | | IP(main line) |
| 300.8 | −4.7 | 296 (1) | −2.1 | 296.1 | −2.0 | 296 (1) | −2.2 | double excitation |
| 304.0 (4) | −7.9 | 303.3 (6) | −10 | 303.7 (6) | −9.6 | 303.1 (6) | −9.3 | $\sigma^*$(C–O) |

[a] Only features with similar assignments to the metal–carbonyl features are reported here. See refs 13 and 60 for a complete tabulation. [b] TV = IP − $E$, where IP is the energy of the main XPS line. [c] Set to the value established by accurate, absolute calibration (ref 61). [d] Calibration relative to $CO_2$ (1s → $\pi^*$: 290.74 eV[58]): $\Delta E$ = −3.04 eV. [e] Calibration relative to $CO_2$: $\Delta E$ = −2.94 eV. [f] Calibration relative to $CO_2$: $\Delta E$ = −3.00 eV. [g] From XPS (ref 10). [h] From XPS (ref 43).

A major topic of recent theoretical and experimental studies of metal–carbonyl systems[1,2,17-24] has been the nature and extent of screening (relaxation) in excited and ionic states of metal carbonyls via metal-to-ligand charge transfers. Plummer et al.[1,2,19,22,23] suggest that screening has a much larger effect on the core *ion* states than any chemical shift associated with bonding to a transition metal. This screening is the origin of the extensive "shake-up" satellites which are very characteristic of the XPS of transition metal carbonyls and surface-adsorbed CO. The "main line" in the XPS of a transition metal carbonyl corresponds to a shielded ionic (*1s*) state which has appreciable mixing with two-hole, one-particle (2h,1p) configurations, primarily of (*1s*,*3d*,$\pi^*$) character. Therefore, the "main-line" does not correspond to the unshielded (*1s*) configuration to which the $\epsilon_{1s}$ orbital energy is normally associated within Koopman's approximation. The Koopmans' $\epsilon_{1s}$ orbital energies are actually given by the first moment of the XPS signal (i.e., the intensity-weighted average of the energies of all lines in the XPS).[2] Plummer et al.[1,2] found that the first moment of the XPS signals of a variety of 3d transition metal carbonyls is identical with that of free CO, within the evaluation uncertainties (±0.5 eV). This suggests that there is very little *chemical* shift (<0.5 eV) in the C 1s and O 1s IPs of carbonyls bound to transition metals, notwithstanding the rather large *relaxation* shift (2–3 eV). A similar situation occurs with regard to the energies of 1s hole states of chemisorbed CO on many surfaces.[17]

In contrast, various groups[15,18,19,24] have noted that metal-to-carbonyl charge transfer plays a much smaller role in the (*C 1s*,$\pi^*$) and (*O 1s*,$\pi^*$) *excited* states. This situation arises because the core hole potential is "self-shielded" by the electron in the $\pi^*$ orbital. The difference in the shielding (relaxation) characteristics of core-excited and core-ionized states is central to our interpretation of these results.

Recently core excitation of chemisorbates and polymers by soft X-rays (NEXAFS) has been used to determine intramolecular bond lengths from the positions of 1s → $\sigma^*$ transitions.[25] The spectra of gaseous compounds have been used extensively both to demonstrate and to calibrate the correlation.[26,27] A major question remains concerning the optimum way to cross-reference surface and gas-phase 1s → $\sigma^*$ energies, in order to take advantage of the large and growing body of gas-phase spectra of molecules of known geometry. The bond length correlation for gas-phase data[26] has been presented in terms of the parameter $\delta_g = E_\sigma$ − IP = −TV, where $E_\sigma$ is the 1s → $\sigma^*$ energy, IP is the ionization potential of the excited core level (XPS main line), and TV is the term value. In principle, subtraction of the IP removes variations caused by the chemical shifts of the 1s energy and thus, within a frozen orbital approximation (i.e., neglecting relaxation and correlation shifts following core excitation), converts $E$(*1s*,$\sigma^*$), a quantity dependent on two levels, to $\approx\epsilon_{\sigma^*}$, an energy solely related to the $\sigma^*$ orbital. Unfortunately, this approach cannot be used whenever there is a large difference in the relaxation (shielding) contributions to the excited (ISEELS, NEXAFS) and ionic (XPS) states, as appears to be the case in metal carbonyls and surface-adsorbed CO. In these situations there is a failure of the previous schemes[28] used to cross-reference $\delta_g$ (that based on the gas-phase spectra of the ligand) and $\delta_s$ (the analogous parameter for the chemisorbed species). The present results, along those of other recent studies of core excitation in gas-phase transition metal carbonyls,[13,19,21,29-32] show that this problem also exists when comparing 1s → $\sigma^*$ energies of CO(g) and gaseous metal carbonyls. The present gas-phase results place the gas-surface referencing problem in sharper focus. Our analysis leads us to propose alternate ways of cross-referencing chemisorbate NEXAFS and free-molecule ISEELS energies in order to exploit the gas-phase data for bond length determination.

Another reason that $Mn_2(CO)_{10}$, $Mn(CO)_5Br$, and $Mn(CO)_5H$ were chosen for study was to look for possible influences of metal–metal bonding on the core excitation spectra. Recently, a study of the core spectra of a number of perfluoro molecules[33] has indicated that molecules with weak bonds (bond energy less than 200 kJ mol$^{-1}$, e.g., the O–F bonds in $F_2O$ and $CF_3OF$) frequently exhibit low-energy features corresponding to core excitations to localized $\sigma^*$ levels associated with the weak bond. The Mn–Mn bond in $Mn_2(CO)_{10}$ has a bond energy of only 151 kJ/mol.[34] Thus the weak bond effect predicts that low-lying features associated with $\sigma^*$(Mn–Mn) will occur in the metal and possibly carbonyl core spectra.

(17) Fuggle, J. C.; Umbach, E.; Menzel, D.; Wandelt, K.; Brundle, C. R. *Solid State Commun.* **1978**, *27*, 65.
(18) Gumhalter, B. *Phys. Rev. B* **1986**, *33*, 5245. Gumhalter, B.; Wadelt, K.; Avouris, Ph. *Phys. Rev. B* **1988**, *37*, 8048.
(19) Plummer, E. W.; Chen, C. T.; Ford, W. K.; Eberhardt, W.; Messmer, R. P.; Freund, H. J. *Surf. Sci.* **1985**, *158*, 58.
(20) Eberhardt, W.; Stöhr, J.; Outka, D.; Madix, R. J. *Solid State Commun.* **1985**, *54*, 493.
(21) Jugnet, Y.; Himpsel, F. J.; Avouris, Ph.; Koch, E. E. *Phys. Rev. Lett.* **1984**, *53*, 198.
(22) Plummer, E. W.; Ford, W. K.; Eberhardt, W.; Messmer, R.; Freund, H.-J. *Surf. Sci.* **1985**, *158*, 58.
(23) Freund, H.-J.; Messmer, R. P.; Speiss, W.; Behner, H.; Wedler, G.; Kao, C. M. *Phys. Rev. B* **1986**, *33*, 5228.
(24) Menzel, D.; Feulner, P.; Treichler, R.; Umbach, E.; Wurth, W. *Phys. Scripta* **1987**, *T17*, 166.
(25) Stöhr, J.; Gland, J. L.; Eberhardt, W.; Outka, D.; Madix, R. J.; Sette, F.; Koestner, R. J.; Döbler, U. *Phys. Rev. Lett.* **1983**, *51*, 2414. Stöhr, J.; Sette, F.; Johnson, A. L. *Phys. Rev. Lett.* **1984**, *53*, 1684. Stöhr, J. In *X-ray Absorption: Principles, Applications, Techniques of EXAFS, SEXAFS and XANES*; Koningsberger, D., Prins, R. L., Eds.; Wiley: New York, 1987.
(26) Sette, F.; Stöhr, J.; Hitchcock, A. P. *J. Chem. Phys.* **1984**, *81*, 4906.
(27) Outka, D.; Stöhr, J. *Phys. Rev. B* **1987**, *35*, 4119.
(28) Stöhr, J.; Sette, F.; Johnson, A. L. *Phys. Rev. Lett.* **1984**, *53*, 1684.
(29) Eberhardt, W. *Phys. Scripta* **1987**, *T17*, 28.
(30) Eberhardt, W.; Plummer, E. W.; Lyo, E. W.; Reininger, R.; Carr, C.; Ford, W. K.; Sondericker, D. *Aust. J. Phys.* **1986**, *39*, 633.
(31) Eberhardt, W.; Chen, C. T.; Ford, W. K.; Plummer, E. W. *Surf. Sci.* **1985**, *4*, 50.
(32) Morin, P.; Simon, M.; Nenner, I., unpublished results.
(33) McLaren, R.; Ishii, I.; Hitchcock, A. P.; Robin, M. B. *J. Chem. Phys.* **1987**, *87*, 4344.
(34) Chowdhury, D. M.; Poe, A.; Sharma, K. R. *J. Chem. Soc., Dalton Trans.* **1977**, 2352. Goodman, J. L.; Peters, K. S.; Vaida, V. *Organometallics* **1986**, *5*, 815.

Table II. Energies ($E$, eV), Term Values (TV, eV), and Proposed Assignments for Features in the O 1s Spectra of CO, $Mn_2(CO)_{10}$, $Mn(CO)_5Br$, and $Mn(CO)_5H$

| CO[a] | | $Mn_2(CO)_{10}$ | | $Mn(CO)_5Br$ | | $Mn(CO)_5H$ | | assignment |
|---|---|---|---|---|---|---|---|---|
| $E$ | TV[b] | $E$ | TV[b] | $E$ | TV[b] | $E$ | TV[b] | (final orbital) |
| 534.11[c] | 8.3 | 533.78[d] | 5.8 | 533.83[e] | 6.6 | 533.9(1)[f] | 6.1 | $\pi^*$ |
| | | 535.5 | 4.1 | 536.2 | 4.2 | 537.4 | 2.6 | $\pi^*$(delocal) |
| 542.4 | | 539.6[g] | | 540.4[h] | | 540.0[g] | | IP(main line) |
| 550.9 | −8.5 | 549.7 | −10.1 | 549.7 | −9.3 | 549.5 | −9.7 | $\sigma^*$(C–O) |

[a] Only features with similar assignments to the metal carbonyl features are reported here. See refs 13 and 60 for a complete tabulation. [b] TV = IP − $E$, where IP is the energy of the main XPS line. [c] Set to the value established by accurate, absolute calibration (ref 61). [d] Calibration relative to $O_2$ (1s → $\pi^*$: 530.8 eV (ref 39): $\Delta E$ = +2.97 eV. [e] Calibration relative to $O_2$: $\Delta E$ = +3.03 eV. [f] Calibration relative to $O_2$: $\Delta E$ = +3.10 eV. [g] From XPS (ref 10). [h] From XPS (ref 43).

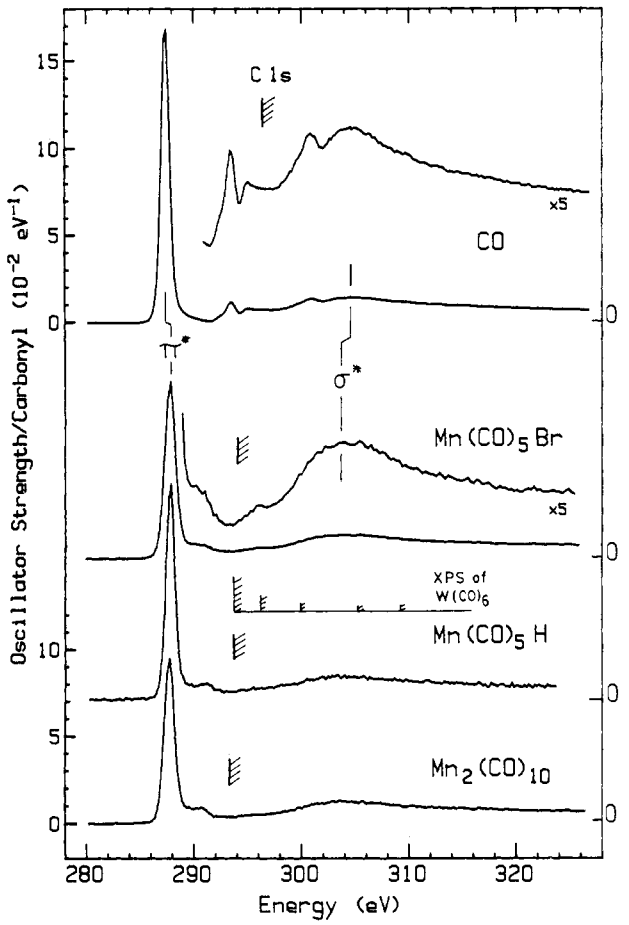


Figure 1. Oscillator strengths per carbonyl for C 1s excitation of CO, $Mn(CO)_5Br$, $Mn(CO)_5H$, and $Mn_2(CO)_{10}$, derived from electron energy loss spectra recorded with 2.5-keV final electron energy, 2° scattering angle, and 0.7-eV fwhm resolution. After background subtraction to isolate only the 1s signal, the spectra were corrected for a kinematic term and normalized at IP + 25 eV to scaled, calculated atomic oscillator strengths, according to a procedure previously documeted.[37] The hatched lines indicate the energies of the main-line C 1s IPs as determined by XPS.[10] The positions and relative intensities of lines in the XPS spectrum of $W(CO)_6$[2] are indicated. Similar, dispersed sets of *C 1s* ion states are expected for the Mn compounds. Note that the shake-up and shake-off signals of CO are negligible on the same vertical scale.[22]

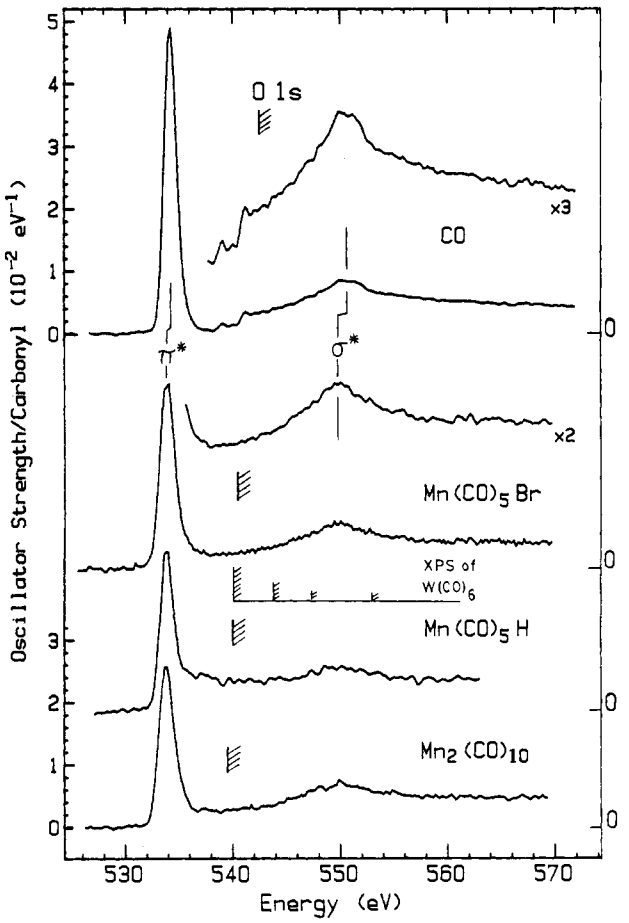


Figure 2. Oscillator strengths per carbonyl for O 1s excitation of CO, $Mn(CO)_5Br$, $Mn(CO)_5H$, and $Mn_2(CO)_{10}$, derived from ISEELS. See caption to Figure I for further details.

## II. Experimental Section

The inner-shell electron energy loss spectrometer and operating techniques have been described previously.[35] The spectra were obtained using 2.5-keV final electron energy, 2° scattering angle, and 0.6-eV fwhm resolution. $Mn_2(CO)_{10}$ and $Mn(CO)_5Br$ samples were used as supplied from Strem Chemicals. $Mn(CO)_5H$ was prepared according to the method of King.[36] The low vapor pressure of the solid compounds required the use of a direct inlet system with placement of the sample as close as possible to the scattering region.

The C 1s and O 1s spectra were converted to absolute optical oscillator strengths ($f$ values) using a conversion procedure described and tested previously.[37] In the present work we wish to interpret rather small shifts in ($1s,\pi^*$) oscillator strengths per carbonyl group. Thus the limits of precision and accuracy become important. We estimate a precision of 5% based on repeat analyses of independent data sets. Systematic effects place rather larger limits on the absolute accuracy of the oscillator strengths; comparison to other measurements[14] suggests 20%. The accuracy is limited by reproducibility of the spectrometer transmission function, errors in the assumption of atomic-like continuum intensities at 25 eV above the IP, and the accuracy of the function chosen to extrapolate the pre-edge background to IP + 25 eV. A possible additional uncertainty particular to this work is associated with the choice of IP. Systematic effects of about 5% are found if the 1s IPs of free CO, which are approximately equal to the first moment IPs of the metal carbonyls,[2] rather than the energies of the main XPS line of the transition metal carbonyl, are used to map calculated atomic values onto the experimental continuum intensities.

(35) Hitchcock, A. P.; Beaulieu, S.; Steel, T.; Stöhr, J.; Sette, F. *J. Chem. Phys.* **1984**, *80*, 3927.

(36) King, R. B. *Organometallic Synthesis*; Academic Press: New York, 1965; Vol. 1, pp 158–160.

(37) McLaren, R.; Clark, S. A. C.; Ishii, I.; Hitchcock, A. P. *Phys. Rev. A* **1987**, *36*, 1683.

## III. Results and Discussion

**1. C 1s and O 1s Spectra.** The C 1s and O 1s oscillator strength spectra of CO and the three manganese carbonyls are shown in Figures 1 and 2, while the energies, term values, and proposed assignments are presented in Tables I and II. Note that the constant vertical scales of Figures 1 and 2 refer to oscillator strength per carbonyl; the actual $f$ values for $Mn(CO)_5L$ (L = H or Br) and $Mn_2(CO)_{10}$ are obtained by multiplying by 5 or 10. The C 1s and O 1s IPs indicated are the main-line XPS energies.[10]

As has been found in previous studies of core excitation in metal carbonyls,[13,14,19,21,29-32] the $\pi^*$ and $\sigma^*$ resonances dominate the core excitation spectra of the manganese carbonyls, and the spectra are remarkably similar to those of free CO. This is in distinct contrast to the core excitation spectra of solely $\pi$-bonded systems such as the metallocenes, where the near edge features change dramatically with identity of the metal.[38] Close inspection of Figures 1 and 2 reveals appreciable differences between CO and the Mn carbonyls in the region between the $\pi^*$ and $\sigma^*$ resonances. The sharp Rydberg and double excitation structures present in this region of the spectrum of free CO are quenched, while additional weak bands are introduced around 291 eV (C 1s) and 537 eV (O 1s), just above the $\pi^*$ resonance. Possible assignments for the features just above the $\pi^*$ peak include $1s \rightarrow \pi^*$(delocal),[13] $1s \rightarrow \sigma^*$ (Mn–C), $1s \rightarrow$ Mn 4p, or $1s \rightarrow$ Rydberg transitions. Contributions from both the first and the second of these possibilities seem the most likely. The greater intensity of the 291-eV C 1s feature than the 537-eV O 1s feature supports a $1s \rightarrow \sigma^*$(Mn–C) assignment since the overlap of $\sigma^*$(Mn–C) and O 1s orbitals would be small. At the same time there are several unoccupied $\pi^*$ orbitals in these compounds and 1s excitations to these higher energy $\pi^*$ orbitals are dipole allowed. Ground-state calculations, supported by valence excitation spectra, indicate that $Mn(CO)_5L$ has three groups of $\pi^*$ orbitals spread over 2.5 eV,[6] while the $\pi^*$ orbitals of $Mn_2(CO)_{10}$ span a region of 1.5 eV.[39] Recently Frank et al.[40] have reported the coverage dependence of the inverse photoemission spectra of CO/Ni(111). Above 0.2 ML (ML = monolayer) coverage $\pi^*$ features are observed over a 3.9-eV range. The existence and large energy separation of the multiple $\pi^*$(CO) orbitals was attributed to overlap of the $\pi^*$'s of adjacent CO molecules, an interaction similar to that leading to splitting of the $\pi^*$ orbitals of transition metal carbonyls. We note that this splitting will have a much smaller effect on the core excitation spectrum because of the strong localization effect of the core hole. Thus, as Cooper et al.[13] have discussed, the main $1s \rightarrow \pi^*$ resonances (287, 531 eV) correspond to population of the lowest energy $\pi^*$ orbital, that which is localized on the core-excited carbonyl. Core excitations to $\pi^*$(delocal), i.e., higher energy $1s \rightarrow \pi^*$ transitions, are essentially charge transfers onto other carbonyls, and these will have very low intensity because of poor spatial overlap.

In the region between the C 1s IP and the maximum of the C $1s \rightarrow \sigma^*$ resonance, the spectra of the manganese–carbonyl complexes do not exhibit the sharp double excitation features seen around 301 eV in free CO (Figure 1). Instead there is a broad shoulder at ≈296 eV, below the $\sigma^*$(C–O) resonances. Similar, but better defined, continuum onset features were observed by Cooper et al.[13] in the corresponding regions of the C 1s and O 1s spectra of $Ni(CO)_4$. These near-continuum features are probably two-electron excitations (perhaps of metal → ligand charge-transfer character). The much broader character of these supposed two-electron transitions (relative to those of CO, where vibrational structure has been resolved[41]) parallels the disappearance of the Rydberg structure, which is weakened and/or broadened into invisibility by the increased molecular size and mixing with other virtual orbitals. Based on these two aspects one might generalize that broad features are characteristic of inner-shell spectra of metal carbonyls. However, this is not true since vibrational structure has been resolved in the $C1s \rightarrow \pi^*$ transition of $Ni(CO)_4$.[13]

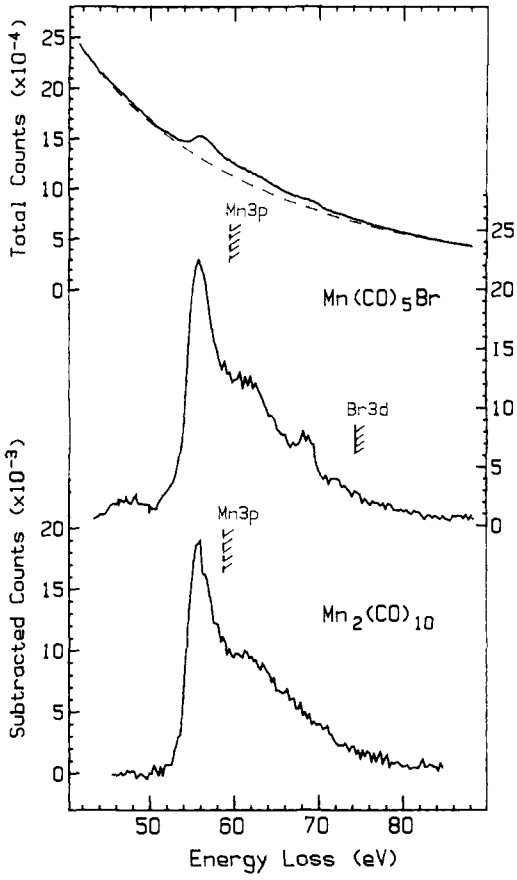


**Figure 3.** Electron energy loss spectra of $Mn(CO)_5Br$ and $Mn_2(CO)_{10}$ in the region of Mn 3p (and Br 3d) excitation. The middle trace displays the difference between the two curves shown in the upper portion of the plot (solid, raw data; dashed, subtracted background). The Mn 3p IPs (vertical dashed lines) are estimated by requiring equal term values of the Mn 3p → 3d and Mn $2p_{3/2}$ → 3d resonances.

Based on analogies with the spectra of some weakly bound perfluoro compounds,[13] a low-lying "$\sigma^*$(Mn–Mn)" level is expected in $Mn_2(CO)_{10}$, associated with the weak Mn–Mn bond (151 ± 2.1 kJ/mol[34]). According to the ground-state MO scheme of Levinson and Gray,[39] the $\sigma^*$(Mn–Mn) orbital is a $d_{z^2}$ $6b_2$ orbital. C 1s or O 1s excitations to $d_{z^2}$ $6b_2$ are dipole-allowed; however, the C 1s or O 1s spectra of $Mn_2(CO)_{10}$ show no evidence of low-energy features additional to those in $Mn(CO)_5L$. The apparent weakness of X 1s → Mn 3d transitions (X = C, O) is somewhat surprising. The molecular symmetry allows such transitions; $C1s \rightarrow e_{1g}(d_{xz},d_{yz})$ are seen in the metallocenes,[38] and the main features of the C 1s and N 1s energy loss spectra of solid transition metal nitrides and carbides are assigned as 1s → M 3d excitations.[42] The absence of such ligand → metal, 1s → 3d charge-transfer bands in the C 1s or O 1s spectra of the manganese carbonyls must reflect a strong spatial and energetic separation of the metal-based virtual orbitals and the ligand core levels in neutral carbonyl complexes. The difference between the carbonyl complexes and the carbides may be related to the differences between molecular and extended ionic bonding.

**2. Mn 3p and Mn 2p Spectra.** The Mn 3p and Mn 2p spectra of $Mn_2(CO)_{10}$ and $Mn(CO)_5Br$ are shown in Figures 3 and 4 while the energies, term values, and proposed assignments are presented in Table III. The Mn 2p and Mn 3p spectra of $Mn(CO)_5H$ are

(38) Rühl, E.; Hitchcock, A. P. *J. Am. Chem. Soc.*, accepted for publication.
(39) Levinson, R. A.; Gray, H. B. *J. Am. Chem. Soc.* **1975**, *97*, 6042.
(40) Frank, K. H.; Sagner, H. J.; Koch, E. E.; Eberhardt, W. *Phys. Rev. B* **1988**, *38*, 8501.
(41) Shaw, D. A.; King, G. C.; Cvejanovic, D.; Read, F. H. *J. Phys. B* **1984**, *17*, 2091.
(42) Pflüger, J.; Fink, J.; Crecelius, G.; Bohnen, K. P.; Winter, H. *Solid State Commun.* **1982**, *44*, 489. Pflüger, J.; Fink, J.; Schwarz, K. *Solid State Commun.* **1985**, *55*, 675.

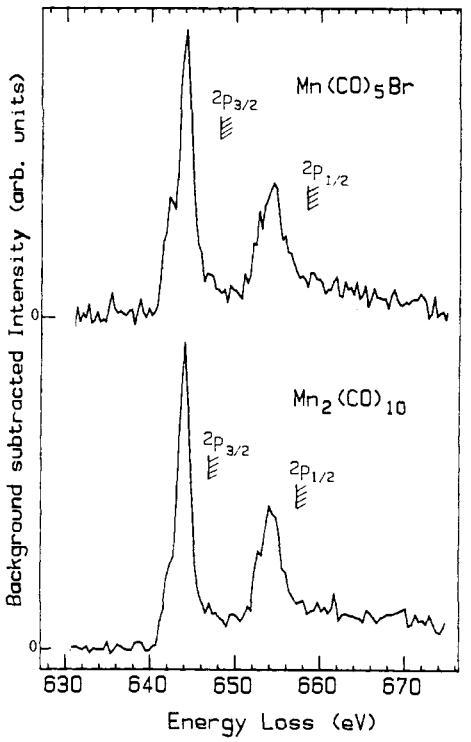


**Figure 4.** Electron energy loss spectra of $Mn(CO)_5Br$ and $Mn_2(CO)_{10}$ in the region of Mn 2p excitation. A linear background has been subtracted. Hatched lines indicate the Mn 2p IPs from XPS.[43]

expected to be similar to those of $Mn_2(CO)_{10}$. Unfortunately, only the Mn 2p IPs have been published.[43] The Mn3p IP's have been estimated by assuming identical term values for the main 2p → 3d and Mn 3p → 3d excitations.

**a. Mn 3p.** In the case of the weak Mn 3p spectra, curved backgrounds, obtained by fitting the pre-edge valence ionization continuum, have been subtraced to better visualize the 3p signal. Comparison of the accumulated and background subtracted counts (Figure 3) reveals the difficulties of obtaining good statistics on the Mn 3p spectra even though the total signal rate at these relatively low energy losses is quite high. As with the 3p spectra of atomic Mn[44] and other 3d transition metal vapors,[45] the spectrum is dominated by the 3p → 3d giant resonance feature which is intense because of excellent same-shell dipole overlap, but also very broad on account of multiplet effects and the large natural line width (≈1 eV) associated with the Coster–Kronig decay of the 3p level. The $3p_{3/2}$–$3p_{1/2}$ spin–orbit splitting (ca. 0.4 eV[44]) is masked by the large natural line widths. The manganese carbonyl 3p → 3d resonance is shifted almost 5 eV above that in atomic Mn, indicating a large Mn 3p chemical shift. The spectrum of atomic Mn[44] exhibits several sharp 3p → 4s transitions around 48–49 eV. There is at best only weak, broad structure in the corresponding region (52–53 eV) of the Mn carbonyl spectra, consistent with a quenching of Rydberg structure with addition of the ligands. The broad maxima around 63 eV in the Mn 3p continua correspond to the rather sharp (*3p*,*3d*,3d) double exctitation and shake-up structure observed around 57 eV in the atomic Mn spectrum. Again these Rydberg-like features, which are sharp in the atomic spectra, appear to be broadened and partially quenched by the ligands.

There is a peak at 69 eV in the spectrum of $Mn(CO)_5Br$ (Figure 3) which does not have an equivalent in the spectrum of $Mn_2(CO)_{10}$. This feature is assigned to Br 3d → σ*(Mn–Br) excitations with a term value of 6.4 eV relative to the Br $3d_{5/2}$ IP of 74.3 eV.[43] Previous Br 3d spectra[46–48] have consistently exhibited broad σ* features in the discrete along with a very broad maximum around 110 eV associated with the 3d → εf continuum, which has a delayed onset due to the centrifugal barrier. Although the 100–130-eV region was studied in detail (spectra not shown), the rapid change in background and the relatively small contribution of the Br 3d signal to the total spectrum do not allow us to make a positive identification of the expected Br 3d → εf continuum feature.

**Table III.** Energies (*E*, eV), Term Values (TV, eV), and Proposed Assignments for Features in the Mn 3p and Mn 2p Spectra of $Mn_2(CO)_{10}$ and $Mn(CO)_5Br$

| $Mn_2(CO)_{10}$ | | | $Mn(CO)_5Br$ | | | assignment (final orbital) | |
|---|---|---|---|---|---|---|---|
| | TV | | | TV | | | |
| *E* | 3/2 | 1/2 | *E* | 3/2 | 1/2 | 3/2 | 1/2 |
| | | | Mn 2p | | | | |
| 642.3 | 4.7 | | 642.3 | 5.6 | | 3d | |
| 644.0[c] | 3.0 | | 644.0[c] | 3.9 | | 3d | |
| 647.0 | | | 647.94 | | | $2p_{3/2}$ IP[a] | |
| 652.8 | | 4.6 | 652.8 | | 5.6 | | 3d |
| 654.2 | | 3.2 | 654.2 | | 4.2 | | 3d |
| 657.4 | | | 658.4 | | | | $2p_{1/2}$ IP[b] |

| | | Mn 3p[d] | | |
|---|---|---|---|---|
| *E* | TV | *E* | TV | assignment (final orbital) |
| 55.8[f] | (3.0) | 55.7[f] | (3.9) | 3d |
| 58.8 | | 59.6 | | IP[e] |
| 63.0(5) | (4.2) | 61.7 (5) | (2.1) | double excitation |
| | | Br 3d[g] | | |
| | | 67.9(5) | 6.4 | σ*(Mn–Br) |
| | | 74.3 | | $3d_{5/2}$ IP[h] |

[a] From XPS (ref 10 and 43). [b] Separation of peaks 2 and 4 was added to the $2p_{3/2}$ IP to get the $2p_{1/2}$ IP. [c] Calibrated relative to 1s → π* of $O_2$ (530.8 eV): $\Delta E$ = 112.8 (2) eV. [d] The Mn $3p_{3/2}$ and $3p_{1/2}$ components are not resolved since the spin–orbit splitting (ca. 0.4 eV) is smaller than the natural line width (≈1 eV). [e] Average 3p IP estimated by assuming identical 3p → 3d and 2p → 3d term values. [f] Calibrated relative to 1s → π* of $CO_2$ (290.74 eV): $\Delta E$ = 235.4 (2) eV for $Mn_2(CO)_{10}$; $\Delta E$ = 235.2 (5) eV for $Mn(CO)_5Br$. [g] Br $3d/_{5/2}$ and $3d_{3/2}$ components separated by the spin–orbit splitting of ≈1.1 eV are expected but are not resolved due to the limited statistics. [h] Ionization potential of the Br $3d_{5/2}$ component from ref 43.

**b. Mn 2p.** The Mn 2p spectra of $Mn_2(CO)_{10}$ and $Mn(CO)_5Br$ shown in Figure 4 have had a linear background subtracted which was about the same size as the maximum excursion of the plotted signal. The poor statistics of these spectra are related to the intrisic weakness of ISEELS signal at high energy losses as well as the limited vapor pressure that could be obtained with an unheated collision cell. The Mn 2p spectrum of atomic Mn has not been reported to our knowledge. However, the photoabsorption spectrum of Mn phthalocyanine in the region of the Mn $2p_{3/2}$ threshold has been published.[49] As with the Mn 3p spectra, the Mn 2p spectra of $Mn_2(CO)_{10}$ and $Mn(CO)_5Br$ are very similar. They are dominated by the strong 2p → 3d resonances, in each case with a low-energy shoulder, presumably reflecting a split Mn 3d manifold. The higher energy $2p_{1/2}$ → 3d transitions appear to be somewhat broader (by about 20%), as expected from the aditional super-Coster–Kronig decay of the Mn $2p_{1/2}$ hole, allowed because of the large spin–orbit splitting (10 eV). The absolute energies of the Mn 2p → 3d and Mn 3p → 3d resonances of the two compounds are very similar even though there is almost a 1-eV chemical shift of the 2p IP associated with the electronegative bromide ligand. This indicates that the Br ligand shifts both the

(43) Avanzino, S. C.; Chen, H. W.; Donahue, C. J.; Jolly, W. L. *Inorg. Chem.* **1980**, *19*, 2201.
(44) Bruhn, R.; Sonntag, B.; Wolff, H. W. *Phys. Lett. A* **1978**, *69*, 9. Cooper, J. W.; Clark, C. W.; Cromer, C. L.; Lucarto, T. B.; Sonntag, B. F.; Tomkins, S. *Phys. Rev. A* **1987**, *35*, 3970.
(45) Schmidt, E.; Schroeder, H.; Sonntag, B.; Voss, H.; Wetzel, H. E. *J. Phys. B* **1985**, *18*, 79. Meyer, M.; Prescher, Th.; von Raven, E.; Richter, M.; Schmidt, E.; Sonntag, B.; Wetzel, H. E. *Z. Phys. D* **1986**, *2*, 347.
(46) Hitchcock, A. P.; Brion, C. E. *J. Electron Spectrosc., Relat. Phenom.* **1978**, *13*, 193.
(47) Shaw, D. A.; Cjevanovic, D.; Read, F. H. *J. Phys. B* **1984**, *17*, 1173.
(48) Morin, P.; Nenner, I. *Phys. Scripta* **1987**, *T17*, 171.
(49) Koch, E. E.; Jugnet, Y.; Himpsel, F. J. *Chem. Phys. Lett.* **1985**, *116*, 7.

**Table IV.** Energies ($E$, eV), Term Values (TV, eV), and Shifts Relative to Free CO ($\Delta E_{\pi^*}$,[d] eV) for 1s → $\pi^*$ Transitions in Transition Metal Carbonyls

| species | C 1s energies (eV) | | | O 1s energies (eV) | | |
|---|---|---|---|---|---|---|
| | $E$ | TV | $\Delta E_{\pi^*}$ | $E$ | TV | $\Delta E_{\pi^*}$ |
| CO | 287.40 | 8.69 | | 534.11 | 8.3 | |
| $Fe(CO)_5$[b] | 287.7 | 5.7 | 0.28 | 533.4 | 6.0 | −0.7 |
| $Fe_2(CO)_9$[b] | 287.9 | 5.5 | 0.48 | 533.1 | 6.3 | −1.0 |
| $Mn_2(CO)_{10}$ | 287.73 | 5.57 | 0.30 | 533.8 | 5.8 | −0.36 |
| $Mn(CO)_5H$ | 287.85 | 5.95 | 0.31 | 533.9 | 5.9 | −0.21 |
| $Mn(CO)_5Br$ | 287.97 | 6.13 | 0.33 | 533.9 | 6.5 | −0.21 |
| $Cr(CO)_6$[c] | 287.58 | 5.63 | 0.18 | 533.85 | 5.64 | −0.26 |
| $Mo(CO)_6$[c] | 287.55 | 5.61 | 0.15 | 533.77 | 5.82 | −0.33 |
| $Ni(CO)_4$[c] | 287.61 | 6.17 | 0.21 | 533.93 | 6.18 | −0.18 |

[a] $\Delta E_{\pi^*}$ = coordinated CO − free CO. [b] From synchrotron photoyield measurements quoted in ref 19. The $\Delta E_{\pi^*}$ values are considerably larger than found in the energy loss work, suggesting possible problems with accuracy of energy scale calibrations. [c] Electron energy loss results (refs 13 and 14).

Mn np and 3d levels by similar amounts.

The 2p and 3p spectra of $Mn_2(CO)_{10}$ do not exhibit any features with term values greater than 6 eV, i.e., below those seen in $Mn(CO)_5Br$. This is surprising in the context of the weak-bond model.[33] The MO schemes of $Mn(CO)_5L$[6] and $Mn_2(CO)_{10}$,[39] derived from calculation and UV spectroscopy, indicate that the $6b_2$ $\sigma^*$(Mn–Mn) in $Mn_2(CO)_{10}$ should lie 1.5 eV lower than the corresponding $d_{z^2}$ orbital in $Mn(CO)_5L$. However, the $d_{z^2}$ $6b_2$ $\sigma^*$(Mn–Mn) is accessible by dipole excitation from only one of the six np orbitals. The apparent absence of an additional low-lying transition in the Mn np spectra of $Mn_2(CO)_{10}$ relative to those of $Mn(CO)_5Br$ may simply be a consequence of the limitations of dipole selection rules, combined with the limited statistical precision of our results.

**3. 1s → $\pi^*$ Energies and Oscillator Strengths: ($d\pi$–$p\pi^*$) Back-Bonding. a. "Term Values".** The absolute energies, term values, and energy shifts for the 1s → $\pi^*$ transitions in a variety of transition metal carbonyls are presented in Table IV. The large shift (≈2–3 eV) in the C 1s and C 1s IPs of the metal carbonyls relative to free CO has been interpreted[10] in terms of an electrostatic chemical shift. If this is so, and if one references the ($1s,\pi^*$) energies to the main XPS line, then the relatively similar 1s → $\pi^*$ energies of CO and the metal carbonyls imply a chemical shift of ≈2 eV in $\epsilon_{\pi^*}$. However, if the shifts in the main line XPS energies are due mainly to relaxation effects, then the conventional calculation of term values relative to the lowest energy $1s$ ion state will overestimate the chemical shift. Instead, the first moment of the XPS should be used as the ionization limit. Since there are intense shake-up satellites in the metal–carbonyl XPS (see the data for $W(CO)_6$[2] plotted in Figures 1 and 2), there is an appreciable energy difference between the main XPS line and the first moment 1s IP. This amounts to ≈2 eV according to the analyses by Plummer et al.[2] of the XPS spectra of several metal carbonyls. Thus referencing the excitation energies to the first moment IP leads to modified "term values" which imply that $\epsilon_{\pi^*}$ in the metal carbonyls is close to $\epsilon_{\pi^*}$ of free CO. Although the full XPS spectra of the manganese compounds are not available, the "main-line" IPs of all three compounds under study are similar (see Table V). Therefore, given that both the XPS first moments and the 1s → $\pi^*$ energies of most transition metal carbonyls are similar to those of free CO, we conclude that the $\pi^*$ energies ($\epsilon_{\pi^*}$) of transition metal carbonyls are within 0.5 eV of those of free CO.

Small but accurately measurable shifts ($\Delta E_{\pi^*}$) are observed in the 1s → $\pi^*$ energies of the transition metal carbonyls relative to free CO [ca. +0.3 eV (C 1s, $\pi^*$) and −0.2 eV (O 1s, $\pi^*$); see Table IV]. Even larger shifts in 1s → $\pi^*$ excitation energies occur in the core excitation spectra of chemisorbed CO. The shifts in the ($C\ 1s,\pi^*$) and ($O\ 1s,\pi^*$) energies for CO/Ni(100)[21] are ∼0.3 eV (C 1s) and −1.7 eV (O 1s) from the peak maxima, but +0.2 (C 1s) and −1 eV (O 1s) if the centroid of the asymmetric peaks is taken.[22,50] Thus the direction of shifts of the peak centroids is in agreement with the shifts in ($1s,\pi^*$) positions in the Mn carbonyls relative to free CO, although the magnitudes are quite different. The small ($1s,\pi^*$) shifts on metal–carbonyl binding have been interpreted in terms of differential relaxation effects by Avouris et al.[15,50] and also discussed in detail by Plummer et al.,[22] in each case using arguments based on ab initio cluster calculations. In free CO the $\pi^*$ orbital has greater density on the carbon than the oxygen atom. In the O 1s → $\pi^*$ excited state the occupied $1\pi$ orbital becomes polarized toward the oxygen, and thus the $2\pi^*$ orbital becomes more localized on the carbon. This results in additional $d\pi$–$p\pi$ overlap which stabilizes the ($O\ 1s,\pi^*$) state of the metal carbonyl, leading to a lower energy than in free CO. The core hole polarization (relaxation) in the ($C\ 1s,\pi^*$) state shifts the $\pi^*$ orbital in the opposite sense, leading to a higher ($C$ 1s,$\pi^*$) energy than in free CO. Thus differential core hole relaxation can explain the observed, opposite shifts in the ($C\ 1s,\pi^*$) and ($O\ 1s,\pi^*$) energies of Mn carbonyls relative to free CO. Similar shifts are seen in the 1s spectra of other transition metals[13,14,22] (see Table IV) and in chemisorbed CO.[21,50]

Electron transmission (ET) and inverse photoemission (IPE) spectroscopies probe $\pi^*$ energies without the distortions of the core hole and thus may provide independent measures of the sensitivity of $\pi^*$ energies to electronic structure changes associated with metal–carbonyl bonding. The ET spectra of metal–carbonyl compounds[5] are rather complex because of overlap of metal and ligand related signals and thus do not provide a simple probe of the $\pi^*$(CO) orbital. Although IPE spectra of transition metal carbonyls have not yet been reported, the IPE spectra of CO chemisorbed on various metal surfaces[11] exhibit one of more peaks which are attributed to $\pi^*$ orbitals. A rough correlation of IPES $\pi^*$ energies with IR stretching frequencies has been demonstrated, along with a comparison with NEXAFS ($1s,\pi^*$) energies.[11] According to IPES the $\pi^*$ energy is reduced from +1.6 eV in free CO, where the $\pi^*$ orbital is unbound, to values between −0.5 and −3.5 eV in chemisorbed CO, the exact value depending on the surface and strength of chemisorption. This shift is an order of magnitude larger than that for ($1s,\pi^*$) energies. Image potential screening[11] and intermolecular interaction[40] are believed to be major factors in determining the IPES $\pi^*$(CO) shift with chemisorption. At present, it appears that the correlation between IPE and ground-state $\pi^*$ energies is not yet sufficiently well-established to provide an independent check of the conclusions concerning $\epsilon_{\pi^*}$ that we have reached from the core-excitation results.

Differential polarization effects could shift the $\sigma^*$ resonances in a manner analogous to the 1s → $\pi^*$ transitions. However, any such effects are probably masked by the large width of the $\sigma^*$ resonances and thus the associated uncertainty in peak location. In additon the $\sigma^*$ resonances of the Mn carbonyls have a rather larger shift (0.5 to 1.5 eV) relative to CO which is associated with the changed C–O bond length (see section III.4).

It is noteworthy that the *width* of the 1s → $\pi^*$ lines is much greater in chemisorbed CO[21] than in free CO or the transition metal carbonyls, where vibrational structure can be resolved.[13] Broadening associated with the overlap of signals from multiple chemisorption sites as well as complex relaxation processes has been invoked to explain the additional width. The widths of the IPES $\pi^*$ lines[11] are considerably less than the core-excitation (NEXAFS) resonances for corresponding chemisorbed CO systems, suggesting that core hole effects are more important. The large difference in line widths between chemisorbed CO and transition metal carbonyls provides an important caution with regard to using the spectra of metal–carbonyl compounds as models for understanding the spectra of chemisorbed CO.

**b. ($1s,\pi^*$) Oscillation Strengths.** Table V lists the oscillator strength per carbonyl of the $\pi^*$ resonances for a range of transition metal carbonyls, along with the carbonyl stretching frequencies, XPS main-line shifts and derived atomic charges,[11] which provide alternative measures of $d\pi$–$p^*$ back-bonding. The number of systems examined has been expanded beyond the three Mn car-

(50) Bagus, P. S.; Rossi, A. R.; Avouris, Ph. *Phys. Rev. B* **1985**, *31*, 1722. Avouris, Ph.; Bagus, P. S.; Rossi, A. R. *J. Vac. Sci. Technol. B* **1985**, *3*, 1484.

Table V. Oscillator Strengths per Carbonyl ($f$, $\times 10^{-2}$) for 1s → π* Transitions in Transition Metal Carbonyls

| species | $\nu$CO,[b] cm$^{-1}$ | $f$ ($10^{-2}$)[a] C 1s | $f$ ($10^{-2}$)[a] O 1s | XPS IP shifts (ref 10) C 1s eV | C 1s $e^{-}$[c] | O 1s eV | O 1s $e^{-}$[c] |
|---|---|---|---|---|---|---|---|
| CO | 2147 | 17.0 | 6.0 | 0 | 0 | 0 | 0 |
| $Cr(CO)_6$[d] | 2026 | 15.7 | 6.0 | 2.94 | 0.128 | 2.74 | 0.084 |
| $Mo(CO)_6$[d] | 2028 | 10.3 | 4.4 | 2.88 | 0.125 | 2.82 | 0.087 |
| $Mn_2(CO)_{10}$ | 2017 | 11.2 | 4.2 | 2.82 | 0.123 | 2.82 | 0.087 |
| $Mn(CO)_5H$ | 2039 | 12.7 | 4.0 | 2.30 | 0.100 | 2.45 | 0.075 |
| $Mn(CO)_5Br$ | 2063 | 12.2 | 5.2 | 1.96 | 0.085 | 1.97 | 0.061 |
| $Fe(CO)_5$[e] | 2036 | 12.1 | 4.0 | 2.39 | 0.104 | 2.44 | 0.075 |
| $Ni(CO)_4$[d] | 2066 | 8.7 | 4.5 | 2.32 | 0.101 | 2.29 | 0.070 |

[a] Peak areas determined by fits of gaussian peaks to the oscillator strength spectra. In some cases several Gaussians were used to correctly reproduce asymmetric line shapes. The total 1s → π* oscillator strengths may be determined by multiplying the given figure by the number of carbonyls. [b] Degeneracy-corrected frequencies taken from ref 10. [c] Atomic charge at C (O) derived from the indicated shifts in the C 1s (O 1s) main-line IPs relative to free CO (ref 10). [d] Derived from electron energy loss data recorded with 0.3-eV fwhm resolution at the University of British Columbia (refs 13 and 14). Systematic errors associated with different spectrometer transmission functions and the better resolution may exist. [e] Derived from photoion yield data recorded at LURE with 2-eV fwhm resolution (ref 32). These results are of lower accuracy on account of resolution, flux normalization, and calibration limitations.

bonyls by analyzing the inner-shell spectra of five other metal carbonyls obtained in other laboratories.[13,14,32] This has involved digitization and conversion to an absolute oscillator strength scale using atomic continuum normalization.[37] There are somewhat larger uncertainties associated with these latter results since the spectra were recorded using an apparatus with different resolution and transmission functions. We have tested the applicability of our oscillator strength conversion procedures on a digitized spectrum of CO recorded at UBC with higher resolution (fwhm of 0.3 eV).[13] The 1s → π* peak areas agree with the result derived from our spectrum (0.7 eV fwhm resolution) within 10%, indicating that the apparatus transmission functions are not greatly different, at least over the relatively narrow energy range involved in the calibration via atomic continuum normalization. The resolution difference is expected to have negligible effect on the peak *areas* since electron scattering is *not* a resonance process. In contrast, resonant photoabsorption, carried out under conditions where the instrumental line shape is greater than the natural line width, is known to suffer from severe distortions of the oscillator strengths, particularly if absorption saturation occurs.

The virtual orbital accessed in the 288- and 534-eV transitions will be partially located at the metal atom because the π* molecular orbital in a transition metal–carbonyl complex is a linear combination of metal–dπ and ligand–pπ orbitals. Since transition intensities are a spatially weighted dipole overlap, the "charge-transfer" component (1s → Mn 3d) of the 1s → π* excitation will contribute much less than the on-site (at C or O) component (i.e., if one expresses the π*(CO) molecular orbital as a linear combination, $[c_c\phi(\mathrm{C}\ 2p_z) + c_O\phi(\mathrm{O}\ 2p_z) + c_M\phi(\mathrm{M}\ 3d)]$, where $c_C$, $c_O$, and $c_M$ are the expansion coefficients, then the 1s → π* dipole transition matrix element will be given by $c_C\langle \mathrm{X}\ 1s|\mu|\phi(\mathrm{C}\ 2p_z)\rangle + c_O\langle \mathrm{X}\ 1s|\mu|\phi(\mathrm{O}\ 2p_z)\rangle + c_M\langle \mathrm{X}\ 1s|\mu|\phi(\mathrm{M}\ 3d)\rangle$, where, to first order, the atomic transition matrix elements will be compound independent. Since $\langle \mathrm{X}\ 1s|\mu|\mathrm{Mn}\ 3d\rangle \ll \langle \mathrm{X}\ 1s|\mu|\mathrm{X}\ 2p\rangle$, X = C of O, 1s excitations to π* orbitals which have a large metal 3d admixture will be weaker than 1s excitations to π* orbitals which are like free CO). Thus the ($1s,\pi^*$) oscillator strengths in a metal carbonyl should be reduced relative to those in free CO in proportion to the dπ contribution to the π* orbital ($c_M$).

Table V indicates that the oscillator strengths per ligand of the C 1s → π* resonances of the manganese carbonyls are reduced by about 30% relative to those of free CO while those of the O 1s → π* resonances are reduced about 20%. Reduced 1s → π* oscillator strengths also occur in other transition metal carbonyls.[13,14,32] The transitions in $Ni(CO)_4$ are the weakest of all the metal carbonyls studied to date, according to our analysis. The reduction of the O 1s → π* oscillator strength is less than that of the C 1s → π* oscillator strength, consistent with a smaller variation with metal of the $O2p_z$ contribution to the π* orbital. There is a clear trend through the series of metal carbonyls toward reduced $f$ values with increasing number of d electrons. This trend parallels the shifts in the vibrational frequencies (Table V) and thus the relative amounts of dπ–pπ back-bonding.

Qualitatively, all of the observations (i.e., both C 1s and O 1s, all compounds) are as expected if the $f$ values of the 1s → π* transitions are inversely proportional to the extent of back-bonding. It appears that back-bonding has a more direct and a larger influence on the *intensities* than on the *energies* of 1s → π* transitions. Undoubtedly core hole relaxation does influence the intensities; however, it does not appear to influence them as drastically as it does the energies, where the differential relaxation causes opposite shifts in the C 1s and O 1s spectra.

Other studies have also documented a larger influence of back-bonding on the carbon than on the oxygen atom. Relative to free CO, the increase of the carbon 2pπ population for $Ni(CO)_4$ and $Cr(CO)_6$ is ≈0.2 e$^-$ according to Mulliken population analysis[51] and semiempirical CNDO calculations.[52] The oxygen populations are changed by a smaller amount (≈0.05 e$^-$). The correlation of C 1s and O 1s binding energies with carbonyl stretching frequencies[10] predicts average charge transfers of 0.11 e$^-$/CO at the carbon atom and 0.07 e$^-$/CO at the oxygen atom for the species listed in Table V. The ab initio calculations of Beach and Gray[6] indicate a charge transfer of 0.06 e$^-$ in $Mn(CO)_6^+$. SW–X$\alpha$ calculations of $Ni_x(CO)$ clusters predict a Ni 3d → π* transfer of 0.33 e$^-$ for top-site bonded CO.[53] Surface Penning electron spectroscopy of CO adsorbed on Ni(111) surfaces[12] has also been interpreted in terms of dπ–pπ charge transfers. The decreased carbonyl stretching frequencies in metal complexes and surface-adsorbed CO have been correlated quantitatively to back-bonding.[7] All of these considerations predict an increase in back-bonding as the number of d electrons increases, with smaller changes associated with ligand modifications. Thus our results are qualitatively consistent with previous work.

At this stage in our research, we do not feel that detailed quantitative comparisons of these $f$ values with other back-bonding estimates is warranted, given the limited data set and the uncertainties of comparing intensites derived from several different spectrometers. Although it is difficult to obtain oscillator strengths with an absolute accuracy of better than 20%, we estimate that the relative *trends* in a related series all recorded with the same instrument under similar conditions can be determined with a precision of better than 5%. Thus there is promise that core-excitation oscillator strengths can provide a quantitative evaluation of back-bonding in metal carbonyls and related systems even though the differences from compound to compound may be small. More precise data on a larger number of compounds will be required to fully test the hypothesis. The interpretation of the 1s → π*(delocal) contribution and the degree of similarity of the π* orbitals of the core excited and ground states are subjects which need to be addressed in future work.

**4. Correlation of 1s → σ* Energies and Bond Lengths: Influence of the Choice of Reference Energy.** As mentioned in the Introduction, the metal–carbonyl spectra allow a test of correlations between bond length and σ* resonance positions and the ways in which spectral data for free CO, metal-complexed CO, and surface-adsorbed CO can be cross-referenced. Following the original formulation,[26] the correlation with bond length can be expressed in terms of the energy relative to the ionization limit, which gives $\delta_g = E_\sigma - \mathrm{IP}$ for gas-phase and $\delta_s = E_\sigma - \mathrm{BE}$ for surface/solid data. Differences between $\delta_g$ and $\delta_s$ are associated with two factors. First there is a trivial *referencing* shift associated with the custom in solid and surface spectroscopies of reported

(51) Hillier, I. H.; Saunders, V. R. *Mol. Phys.* **1971**, *22*, 1025. Demuynick, J.; Veitland, A. *Theor. Chim. Acta* **1973**, *28*, 241.
(52) Freund, H.-J.; Hohlneicher, G. *Theor. Chim. Acta* **1979**, *51*, 145.
(53) Raatz, F.; Salahub, D. H. *Theochem Surf. Sci.* **1986**, *176*, 219.

**Table VI.** Carbonyl Bond Lengths Predicted from 1s → σ* (C–O) Energies Referenced to the IPs of the Metal Carbonyls and Free CO

| species | ref: main-line IP | | | ref: $E(1s,\sigma^*)$ of CO | | | |
|---|---|---|---|---|---|---|---|
| | $\delta_{C1s}$[a] | $\delta_{O1s}$ | $R_{pred}$[b] | $\delta^*_{C1s}$[c] | $\delta^*_{O1s}$ | $R_{pred}$ | $R$[d] |
| CO | 7.7 | 8.3 | 1.14 | 7.7 | 8.3 | 1.14 | 1.12 |
| $Mn(CO)_5Br$ | 9.6 | 9.3 | 1.10 | 7.6 | 7.3 | 1.16 | 1.14[e] |
| $Mn(CO)_5H$ | 9.3 | 9.7 | 1.10 | 7.0 | 7.1 | 1.18 | 1.142 |
| $Mn_2(CO)_{10}$ | 10.0 | 10.1 | 1.08 | 7.2 | 7.3 | 1.17 | 1.13 |
| $Fe(CO)_5$[f] | 9.3 | 10.2 | 1.08 | 6.4 | 7.6 | 1.18 | 1.145 |
| $Ni(CO)_4$[g] | 10.7 | 10.0 | 1.07 | 8.3 | 7.7 | 1.15 | 1.14 |

[a] $\delta = E_\sigma - IP$, where IP is the energy of the main XPS line (see Tables I and II). [b] $R_{pred}$ determined from the $Z = 14$ correlation line: $\delta_{avg} = 42.19 - 29.81*R$, where $\delta_{avg}$ is the average of $\delta_{C1s}$ and $\delta_{O1s}$. Note that this correlation line involves a small correction of the parameters published in ref 26. [c] $\delta^* = E_\sigma - IP(CO)$. [d] From electron diffraction structures reported in ref 18 and 19. [e] Values of $R_{ax} = 1.16$, $R_{eq} = 1.12$ Å have been predicted from extended Hückel calculations ref 59 (there are no experimental data). The weighted average is quoted here. [f] The value for the C 1s → σ*(C–O) energy in $Fe(CO)_5$ is less accurately determined than those of the other species since there were flux normalization difficulties ref 32. Note that Eberhardt et al.[31] report $E_\sigma$ = 308 eV ($\delta$(C 1s) = 13 eV) for $Fe(CO)_5$. [g] Derived from data tabulated in ref 13.

transition energies relative to the Fermi level (BE) as opposed to the vacuum level (IP) as in gas-phase spectroscopy. This introduces a shift in the $\delta$ scales equivalent to the work function, which is typically 3–6 eV for transition metal surfaces with organic chemisorbates. Second, there are additional shifts in the $\delta$ quantity because of large (3–6 eV) *relaxation* effects of the metal surface on the IP (but not $E_\sigma$) of adsorbed molecules.[1,17-24] Third, there is the possibility of *chemical* shifts related to charge transfers between metal and chemisorbed molecule (*in the ground state*).

The $\delta$ values for 1s → σ* transitions ($E_\sigma$ referenced to the main XPS IP) in a variety of transition metal carbonyls are summarized in Table VI, along with the known C–O bond lengths[54,55] and those predicted from the $\delta_{avg}$ values by application of the bond-length correlation as outlined in ref 26. It is clear that use of this formulation predicts bond lengths which are consistently smaller than the known values. Although the magnitude of the error (0.06 Å) does not greatly exceed the 0.05-Å accuracy claimed[26] for bond lengths deduced from σ* resonances, it is consistently in the *wrong* direction; i.e., it predicts bond shortening relative to free CO rather than the bond lengthening[54,55] which is a well-known consequence of metal–carbonyl bonding. This error is rather disturbing since the transition metal carbonyls would seem to be a case where the bond length correlation concept has good applicability (i.e., there are only small shifts in C–O bond lengths associated with the relatively weak external perturbation of the metal atom).

Comparisons of the ISEEL spectra of free molecules with the NEXAFS spectra of related chemisorbates indicate that, if the molecular geometry does not change, corresponding features occur at essentially identical energies, indicating a negligible relaxation effect of the metal substrate on the excitation energies.[22,56] Similarly the $E_\sigma$'s for the transition metal carbonyls are close to those of CO (Tables I and II). Thus, the 2–3-eV increase in the carbonyl $\delta$ values come almost entirely from the 2–3-eV decrease in the 1s IPs which are the XPS main-line energies. In other words, for CO chemisorbed on 3d transition metals and for gas-phase transition metal carbonyls, there appears to be a distortion of the $\delta_g$ scale caused by the larger dπ → pπ charge transfer that occurs with ionization than with excitation. This effect has already been discussed in the context of the 1s → π* term values (section III.3.). If there are no chemical shifts of the 1s or π* levels, then 1s *excitations* will occur at very similar energy in CO and the metal carbonyls since there will be little relaxation because the electron promoted to the π* or σ* orbital will shield the core hole ("self-shielding"). In contrast, the core *ion states* of metal carbonyls will have much greater relaxation than those of free CO since the C 1s or O 1s hole is "bare". It is interesting to note that the self-shielding that damps the relaxation of core-excited relative to core-ionized states occurs even for the very short-lived ($1s,\sigma^*$) "quasi-bound" states or resonances in the 1s continuum. Thus, although relaxation influences excitation and decay spectroscopies to a greatly different extent, it appears that the extent of relaxation is not strongly dependent on the lifetime of the core excitation. As discussed earlier, the first moment of the *complete* XPS spectrum would be a better "1s" reference energy for purposes of comparison to trends with bond length changes in other $Z = 14$, 1s → σ* energies because it should be independent of relaxation. The systematic errors in bond lengths associated with this distortion of the $\delta_g$ scale can be reduced by a variety of means including:

(1) Application of a common, absolute energy scale for the bond length correlation of gas, transition metal complex, and chemisorbed data. This method has been used in several recent NEXAFS studies.[27] A major limitation of this method is that chemical shifts between reference and "unknown" systems are not taken into account. Thus species with large chemical shifts (e.g., compounds with different numbers of fluoride ligands)[57] cannot be used in this form of the correlation, which must also be restricted to species at a single core edge.

(2) Reference to the first moments of the experimental XPS IPs in all cases. Although this would be the most strictly correct, it is difficult to implement in most cases because of the unavailability of long-range XPS spectra which include the shake-up and shake-off signals.

(3) Reference of the 1s → σ* energies of chemisorbed CO to the 1s IPs of free CO. This option may be generalized to any adsorbate in that one could reference the 1s → σ* energies observed in the NEXAFS of chemisorbates to the *gas-phase* IP of the same or a "chemically similar" molecule. Difficulties could arise if there are large modifications of the molecular structure with chemisorption, in which case the identity of the most suitable reference compound could be ambiguous. Also chemical shifts between the gas-phase model and the surface adsorbate may not always be negligible.

For the manganese carbonyls under study a small shift to lower energy of the 1s → σ* resonances is observed compared to CO (cf. Figures 1 and 2, and Table VI). Using the third of the above methods, one obtains C–O bond lengths of 1.16 ± 0.02 Å (Table VI), in better agreement with the known bond lengths in the transition metal carbonyls[54,55] than the estimates provided by referencing to the main XPS energy. At least some of the residual discrepancy between predicted and actual $R$(CO) may be associated with unaccounted chemical shifts, although the improvements in the predicted $R$ values suggests that these are relatively small.

## IV. Summary

The C 1s, O 1s, Mn 3p, and Mn 2p core-excitation spectra of several manganese carbonyl compounds have been recorded and analyzed. Shifts in 1s → π* excitation energies and 1s → π* oscillator strengths are discussed in relationship to changes in the electronic structure with binding of CO to metals. The ($1s,\pi^*$) oscillator strengths are found to be a potentially sensitive probe of the extent of dπ–pπ back-bonding. The positions of the 1s → σ* continuum resonances highlights the different roles of *relax-*

(54) Landolt-Börnstein *Structure Data of Free Polyatomic Molecules*; Springer: Berlin, 1987; Vol. 15.
(55) Churchill, M. R.; Amoh, K. N.; Wasserman, H. J. *Inorg. Chem.* **1981**, *20*, 1609.
(56) Stöhr, J.; Jaeger, R. *Phys. Rev. B* **1982**, *26*, 4111.
(57) Hitchcock, A. P.; Fischer, P.; McLaren, R. In *Giant Resonances in Atoms, Molecules and Solids*; Connerade, J. P., Esteva, J. M., Karnatak, R. C. Eds., NATO ASI Series B: *151*, 281 (1987).
(58) Hitchcock, A. P.; Ishii, I. *J. Electron Spectrosc. Relat. Phenom.* **1987**, *42*, 11.
(59) Penshah, D. A.; McKinney, R. J. *Inorg. Chem.* **1979**, *18*, 3407.
(60) Hitchcock, A. P.; Brion, C. E. *J. Electron Spectrosc. Relat. Phenom.* **1980**, *18*, 1.
(61) Sodhi, R. N. S.; Brion, C. E. *J. Electron Spectrosc. Relat. Phenom.* **1984**, *34*, 363.

*ation* and *chemical* shifts in determining *1s* ionization energies. Improved means of correlating gas and metal-adsorbed $\sigma^*$ resonance positions with bond lengths are detailed.

**Acknowledgment.** We thank M. B. Robin, I. Ishii, and A. Wen for their assistance in recording and analyzing some of the spectra. We also thank C. E. Brion, K. H. Sze, and G. Cooper for providing preprints and for permission to quote unpublished results. This work was financed by the Natural Science and Engineering Research Council of Canada (NSERC). A.P.H. acknowledges the support of an NSERC university research fellowship.

**Registry No.** $Mn_2(CO)_{10}$, 10170-69-1; $Mn(CO)_5Br$, 14516-54-2; $Mn(CO)_5H$, 16972-33-1.

# Stereoselective Alkylation of Glycine Units in Dipeptide Derivatives: "Chirality Transfer" via a Pivalaldehyde *N,N*-Acetal Center[1]

**Robin Polt[†] and Dieter Seebach***

*Contribution from the Laboratorium für Organische Chemie der Eidgenössischen Technischen Hochschule, ETH-Zentrum, Universitätstrasse 16, CH-8092 Zürich, Switzerland.*
*Received August 18, 1988*

**Abstract:** Dipeptide esters (of glycylglycine, glycylalanine, alanylglycine) and aldehydes (isobutyraldehyde, pivalaldehyde, benzaldehyde) are condensed to (4-oxoimidazolidin-3-yl)acetates and -propionates (**1-3**). Lithium enolates of these derivatives are generated (deprotonation of the ring and/or side-chain $\alpha$-carbonyl positions) with LDA, LDA/LiBr, or LHMDS and alkylated with high diastereoselectivity (products **4**, **6**, **7**). Dipeptides of either *R,R* or *S,S* configuration can be prepared from the glycine-containing precursors. Surprising proton-transfer effects (Schemes VI-IX, XII) are interpreted as a consequence of "intimate complexation" among LDA, LiBr, lithium enolates, and diisopropylamine.

A major challenge for chemists is the successful alkylation of enantiomerically pure compounds without loss of optical activity and the stereoselective introduction of new stereogenic centers. Recently, many synthetic procedures which use chiral auxiliaries to achieve overall enantioselective alkylations have emerged.[2] A major disadvantage in all of these procedures is the necessary recovery and/or the cost of the chiral auxiliaries. Where possible, it is preferable to incorporate chiral building blocks into the product itself. One possibility of manipulating bonds on the one and only stereogenic center of simple chiral compounds without generating achiral intermediates and thus producing racemic mixtures is the reaction with an *achiral* auxiliary, creating a new *temporary* stereogenic center (Scheme I). We have been interested in stereoselective alkylations of functionalized enolates. Previously, we have shown that cyclic *S,O*-, *O,O*-, *O,N*-, and *N,N*-acetals are useful as protecting groups to preserve both the functionality and the chirality of $\alpha$- and $\beta$-heterosubstituted carboxylic acid derivatives during enolization and alkylation ("self-reproduction of chirality", or better, "self-regeneration of stereogenic centers").[3]

Reactions on increasingly complex compounds with more sensitive functionality have been another important goal for many research groups in synthesis. One of our goals has been the use of intact peptides as substrates in enolate reactions. New work with imidazolidinones derived from dipeptide esters has resulted in the discovery of a novel type of "chirality transfer" in which the original stereogenic center can be either retained or inverted during enolization/alkylation with the stereoselectivity induced via an *N,N*-acetal carbon atom to the newly created stereogenic center. In synthetic terms, this means that stereogenic centers may be generated along a peptide backbone.[1] This represents a fundamentally new approach to peptide synthesis.[4]

## Results and Discussion

**Preparation of Imidazolidinones.** We have shown previously that simple imines of glycine amides can be cyclized with anhydrous HCl in MeOH.[3a,b,e] Similar methodology worked well with the pivalaldehyde imine of glycylglycine methyl ester. The resulting imidazolidinone hydrochloride crystallized in high yield and proved to be surprisingly stable, possessing a half-life of ca. 1-2 days in $D_2O$ solution at room temperature. The NH group of the imidazolidinone was protected with Z (Cbz) to give **1** (benzyl chloroformate in $CH_2Cl_2/NEt_3$) (Scheme II).[5]

[†]Present address: Department of Chemistry, University of Arizona, Tucson, Arizona 85721.

(1) A preliminary account of this work has appeared: Polt, R.; Seebach, D. *Helv. Chem. Acta* **1987**, *70*, 1930.

(2) (a) Evans, D. A. In *Asymmetric Synthesis*; Morrison, J. D., Ed.; Academic Press: New York, 1984; Vol. 3, pp 1-110. (b) Lutomski, K. A.; Meyers, A. I. *Ibid.* pp 213-274. (c) Enders, D. *Ibid.* pp 275-339. (d) Bergbreiter, D. E.; Newcomb, M. *Ibid.* 1983; Vol. 2, pp 243-273. (e) McIntosh, J. M.; Leavitt, R. K.; Mishra, P.; Cassidy, K. C.; Drake, J. E.; Chadha, R. *J. Org. Chem.* **1988**, *53*, 1947. (f) Oppolzer, W.; Pedrosa, R.; Moretti, R. *Tetrahedron Lett.* **1986**, *27*, 831. (g) Ikegami, S.; Hayama, T.; Katsuki, T.; Yamaguchi, M. *Tetrahedron Lett.* **1986**, *27*, 3403. (h) Sinclair, P. J.; Zhair, D.; Reibenzpies, J.; Williams, R. M. *J. Am. Chem. Soc.* **1986**, *108*, 1103. (i) Brown, S. L.; Davies, S. G.; Foster, D. F.; Seeman, J. I.; Warner, P. *Tetrahedron Lett.* **1986**, *27*, 623. (j) Marco, J. L.; Poyer, J.; Husson, H.-P. *Tetrahedron Lett.* **1985**, *26*, 3567. (k) Belokon, Y. N.; Bulychev, A. G.; Vitt, S. V.; Struchkov, Y. T.; Batsanov, A. S.; Timofeeva, T. V.; Tsyryapkin, V. A.; Ryzhov, M. G.; Lysova, L. A.; Bakhmutov, V. I.; Belikov, V. M. *J. Am. Chem. Soc.* **1985**, *107*, 4252. (l) Schmierer, R.; Grotemeir, G.; Helmchen, G.; Selim, A. *Angew. Chem., Int. Ed. Engl.* **1981**, *20*, 207. (m) Schöllkopf, U.; Groth, U.; Deng, C. *Angew. Chem., Int. Ed. Engl.* **1981**, *20*, 798.

(3) (a) Seebach, D.; Naef, R. *Helv. Chim. Acta* **1981**, *64*, 2704. (b) Seebach, D.; Boes, M.; Naef, R.; Schweizer, W. B. *J. Am. Chem. Soc.* **1983**, *105*, 5390. (c) Seebach, D.; Naef, R.; Calderari, G. *Tetrahedron* **1984**, *40*, 1313. (d) Seebach, D.; Roggo, S.; Zimmermann, J. *Stereochemistry of Organic and Bioorganic Transformations*; Bartmann, W., Sharpless, K. B., Eds.; VCH: New York, 1985; pp 85-126. (e) Seebach, D.; Juaristi, E.; Miller, D. D.; Schickli, C.; Weber, T. *Helv. Chem. Acta* **1987**, *70*, 237. (f) Seebach, D.; Zimmermann, J.; Gysel, U.; Ziegler, R.; Ha, T.-K. *J. Am. Chem. Soc.* **1988**, *110*, 4763-4778. (g) Seebach, D.; Fitzi, R. *Tetrahedron* **1988**, *44*, 5277.

(4) Ojima and co-workers have used asymmetric [2 + 2] cycloaddition reactions of chiral ketenes and amino ester derived imines to synthesize $\beta$-lactams which were opened to produce dipeptides stereoselectively. Although their system uses a chiral auxiliary *and* a chiral imine, the overall "chirality transfer" is similar: (a) Ojima, I.; Chen, H.-J. C. *J. Chem. Soc., Chem. Commun.* **1987**, 625. Additionally, their $\beta$-lactam esters can be enolized and alkylated: (b) Ojima, I.; Qiu, X. *J. Am. Chem. Soc.* **1987**, *109*, 6537.

(5) The *t*-BOC-protected analogue was also prepared (87% yield from the imidazolidinone hydrochloride, mp 73.0-73.5 °C) and was methylated in the same manner as **1a** to give an analogous product (**4b**, BOC instead of Z, 75% yield, mp 81.5-82.5 °C) with comparable stereoselectivity.

0002-7863/89/1511-2622$01.50/0 